NEW DIFFRACTION DATA

Crystal structure of a second polymorph of germacrone, $C_{15}H_{22}O$

James A. Kaduk [1,2,a)] Stacy Gates-Rector [3] and Thomas N. Blanton [3]
[1]*Illinois Institute of Technology, 3101 S. Dearborn St., Chicago, IL 60616, USA*
[2]*North Central College, 131 S. Loomis St., Naperville, IL 60540, USA*
[3]*ICDD, 12 Campus Blvd., Newtown Square, PA 19073-3273, USA*

The crystal structure of a new polymorph of germacrone has been solved and refined using synchrotron X-ray powder diffraction data and optimized using density functional theory techniques. This polymorph (Form II) crystallizes in space group $C2/c$ (#15) with $a = 26.0073(4)$, $b = 9.84383(10)$, $c = 10.53713(13)$ Å, $\beta = 95.7547(11)°$, $V = 2684.04(3)$ Å^3, and $Z = 8$. The crystal structure is dominated by van der Waals interactions, but four C–H⋯O hydrogen bonds are present. The structure exhibits many similarities to the previously reported Form I polymorph FIQLOG, but is clearly different. The powder pattern has been submitted to ICDD for inclusion in the Powder Diffraction File™ (PDF). © *The Author(s), 2022. Published by Cambridge University Press on behalf of International Centre for Diffraction Data.* [doi:10.1017/S0885715622000057]

I. INTRODUCTION

Germacrone was first isolated in 1927 from the essential oil of *Geranium macrorrhizum* (Rovesti, 1927). Germacrone is a sesquiterpene, a terpene that consists of three isoprene units, and exhibits a range of pharmacological activities, including anti-inflammatory, anticancer, antiviral, anti-androgenic, antioxidant, antimicrobial, antifungal, neuroprotective, and also shows insecticidal activities (PubChem; Kim *et al.*, 2019). The systematic name (CAS Registry Number 6902-91-6) is (3*E*,7*E*)-3,7-dimethyl-10-propan-2-ylidenecyclodeca-3,7-dien-1-one. A two-dimensional molecular diagram is shown in Figure 1.

A crystal structure of germacrone has been reported, herein referred to as Type I (Clardy and Lobkovsky, 1998; CSD Refcode FIQLOG). The structure of a related molecule, isogermacrone, has also been reported (Jacobsson *et al.*, 1985; CSD Refcode DICDOI). The FIQLOG structure is in space group *Pc*, and apparently is an example of a chiral structure formed by a cycloalkene molecule, which does not contain chiral centers (Barrero *et al.*, 2008).

This work was carried out as part of a project (Kaduk *et al.*, 2014) to determine the crystal structures of large-volume commercial pharmaceuticals, and include high-quality powder diffraction data for them in the Powder Diffraction File (Gates-Rector and Blanton, 2019).

II. EXPERIMENTAL

Germacrone was a commercial reagent, purchased from TargetMol (Lot #114635), and was used as-received. The white powder was packed into a 1.5 mm diameter Kapton capillary and rotated during the measurement at ~50 Hz. The powder diffraction pattern was measured at 295 K at beamline 11-BM (Antao *et al.*, 2008; Lee *et al.*, 2008; Wang *et al.*, 2008) of the Advanced Photon Source at Argonne National Laboratory using a wavelength of 0.458133(2) Å from 0.5 to 50° 2θ with a step size of 0.001° and a counting time of 0.1 s per step. The high-resolution powder diffraction data were collected using 12 silicon crystal analyzers that allow for high angular resolution, high precision, and accurate peak positions. A silicon (NIST SRM 640c) and alumina (SRM 676a) standard (ratio Al_2O_3:Si = 2:1 by weight) was used to calibrate the instrument and refine the monochromatic wavelength used in the experiment.

The observed powder pattern does not correspond to that calculated from the room-temperature FIQLOG crystal structure (Figure 2), but the sample does seem to contain the Type I phase as an impurity. The pattern collected in this study was difficult to index. The peaks having $I_{rel} > 4\%$ could be indexed on a C-centered monoclinic unit cell with $a = 26.01319$, $b = 9.84676$, $c = 10.53950$ Å, $\beta = 95.77°$,
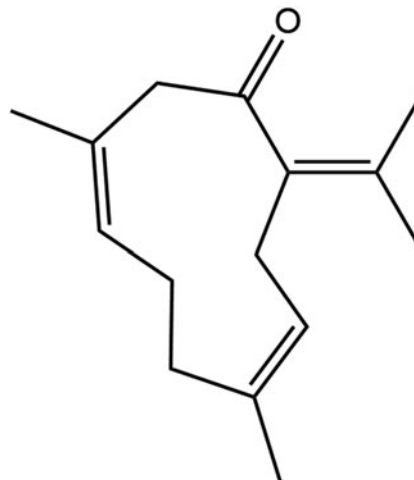
Figure 1. The 2D molecular structure of germacrone.

a)Author to whom correspondence should be addressed. Electronic mail: kaduk@polycrystallography.com
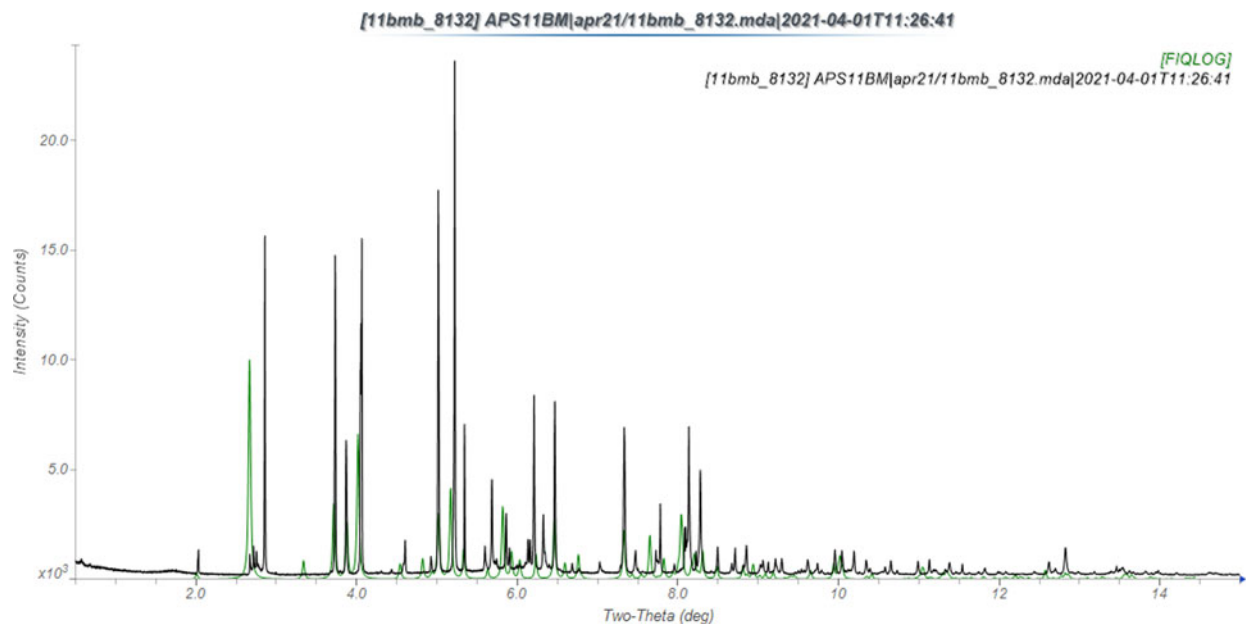
Figure 2. Comparison of the observed synchrotron powder diffraction pattern (black) of germacrone to the pattern calculated from the Form I FIQLOG structure (green).

$V = 2685.98$ Å^3, and $Z = 8$ using JADE Pro (MDI, 2021). The suggested space group was $C2/c$, which was confirmed by successful solution and refinement of the structure. A reduced cell search in the Cambridge Structural Database (Groom *et al.*, 2016) yielded 2 hits, but no structures of germacrone derivatives. Additional unindexed non-FIQLOG peaks suggested the presence of at least one additional crystalline impurity.

A germacrone molecule was extracted from the FIQLOG structure using *Materials Studio* (Dassault, 2021), and saved as a *.mol2 file. The new structure (Type II germacrone) was solved using Monte Carlo simulated annealing techniques

as implemented in EXPO2014 (Altomare *et al.*, 2013). Attempts to solve the structure in space group Cc using two independent molecules yielded significantly worse residuals.

Rietveld refinement was carried out using GSAS-II (Toby and Von Dreele, 2013). Only the 1.0–25.0° portion of the pattern was included in the refinement ($d_{min} = 1.058$ Å). FIQLOG (Type I) was included as a second phase; its concentration refined to 1.3 wt.%. All non-H bond distances and angles were subjected to restraints, based on a Mercury/Mogul geometry check (Bruno *et al.*, 2004; Sykes *et al.*, 2011). The Mogul average and standard deviation for each quantity were used as the restraint parameters. The restraints contributed 5.1% to the
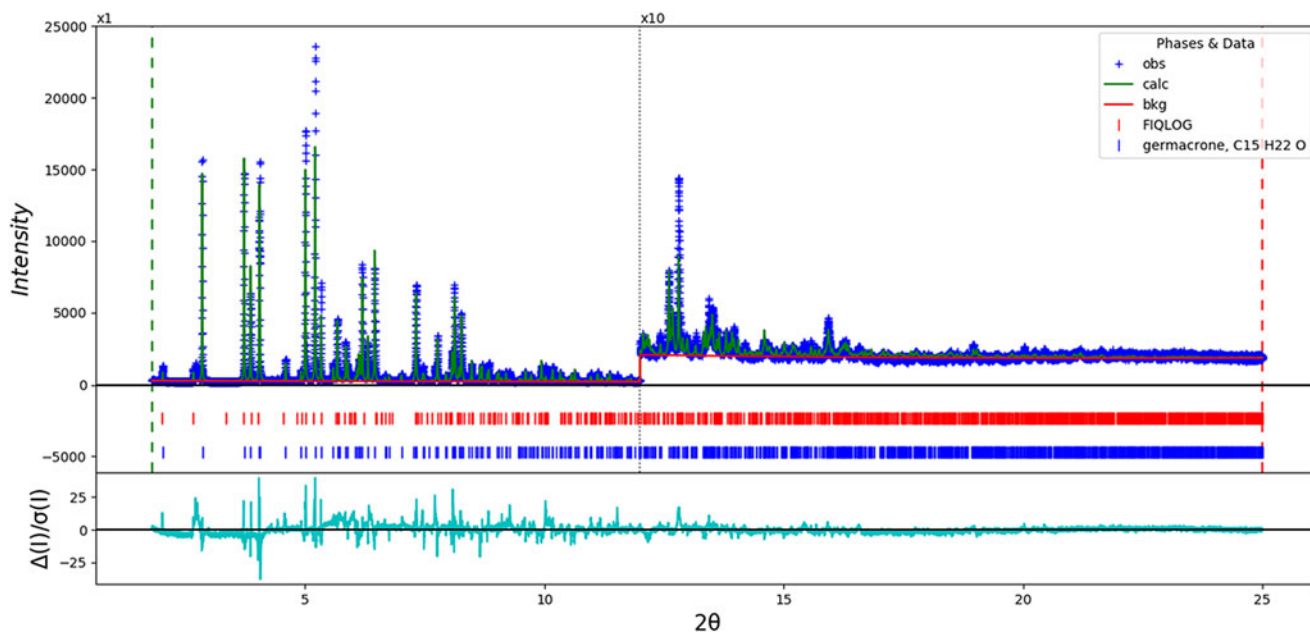
Figure 3. The Rietveld plot for the refinement of germacrone. The blue crosses represent the observed data points, and the green line is the calculated pattern. The cyan curve is the normalized error plot. The vertical scale has been multiplied by a factor of 10× for $2\theta > 12.0°$. The row of blue tick marks indicates the calculated reflection positions for germacrone Form II, and the row of red tick marks indicates the form I FIQLOG peak positions.
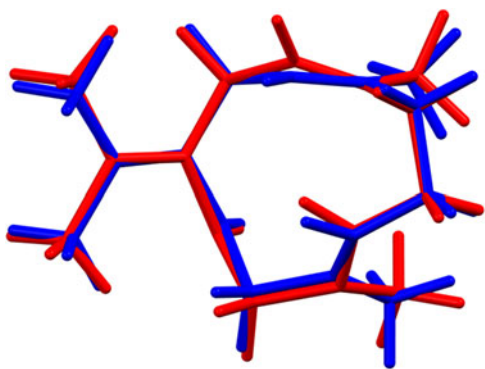
Figure 4. Comparison of the Rietveld-refined (red) and VASP-optimized (blue) structures of the germacrone molecule in Form II. The rms Cartesian displacement is 0.184 Å.

final χ^2. The hydrogen atoms were included in calculated positions, which were recalculated during the refinement using Materials Studio (Dassault, 2021). A single U_{iso} was refined for the C and O atoms. The U_{iso} for the H atoms were fixed at 1.3× the U_{iso} of the heavy atoms to which they are attached. The peak profiles were described using an isotropic microstrain model. The background was modeled using a 3-term shifted Chebyshev polynomial.

The final refinement of 59 variables using 23 237 observations and 37 restraints yielded the residuals R_{wp} = 0.2051 and GOF = 4.02. The residuals are high because the peaks due to

the Type I FIQLOG phase (and presumably also the other impurity peaks) exhibit significant overlap with those of the major phase. The largest peak (0.16 Å from C4) and hole (1.77 Å from O1) in the difference Fourier map were 0.60 and −0.59(15) eÅ^{-3}, respectively. The largest errors in the difference plot (Figure 3) are in the shapes of some of the strong peaks and at the (ignored) impurity peaks.

The crystal structure was optimized using VASP (Kresse and Furthmüller, 1996) (fixed experimental unit cell) through the MedeA graphical interface (Materials Design, 2016). The calculation was carried out on 16 2.4 GHz processors (each with 4 GB RAM) of a 64-processor HP Proliant DL580 Generation 7 Linux cluster at North Central College. The calculation used the GGA-PBE functional, a plane wave cutoff energy of 400.0 eV, and a k-point spacing of 0.5 Å^{-1} leading to a $1 \times 2 \times 2$ mesh, and took ∼5.8 h. A single-point density functional calculation (fixed experimental cell) and population analysis were carried out using CRYSTAL17 (Dovesi *et al.*, 2018). The basis sets for the H, C, and O atoms in the calculation were those of Gatti *et al.* (1994). The calculations were run on a 3.5 GHz PC using 8 k-points and the B3LYP functional, and took ∼2.1 h.

III. RESULTS AND DISCUSSION

The root-mean-square (rms) Cartesian displacement between the Rietveld-refined and DFT-optimized structures is 0.184 Å (Figure 4), within the normal range for correct
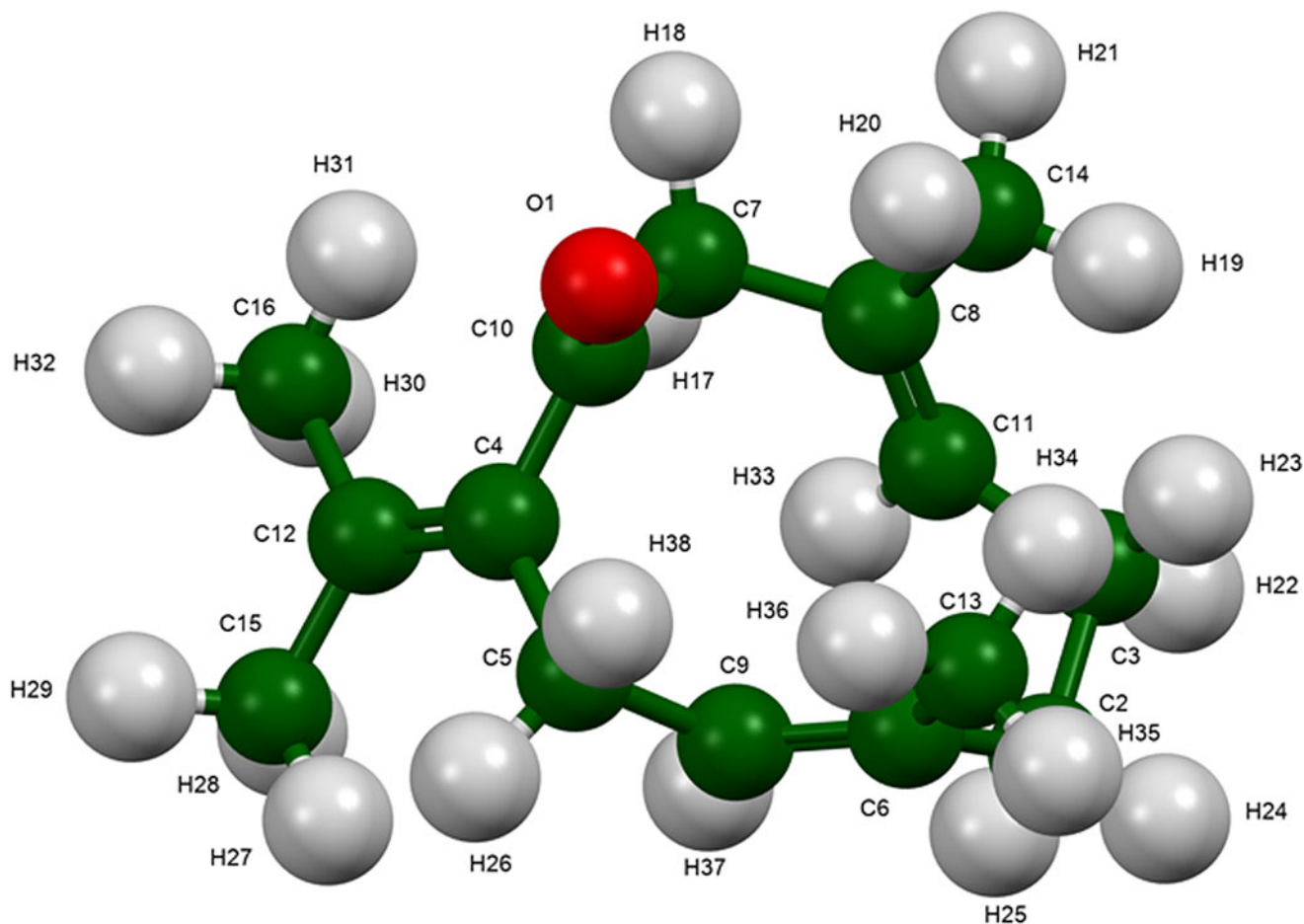
Figure 5. The asymmetric unit of germacrone Form II, with the atom numbering. The atoms are represented by 50% probability spheroids.
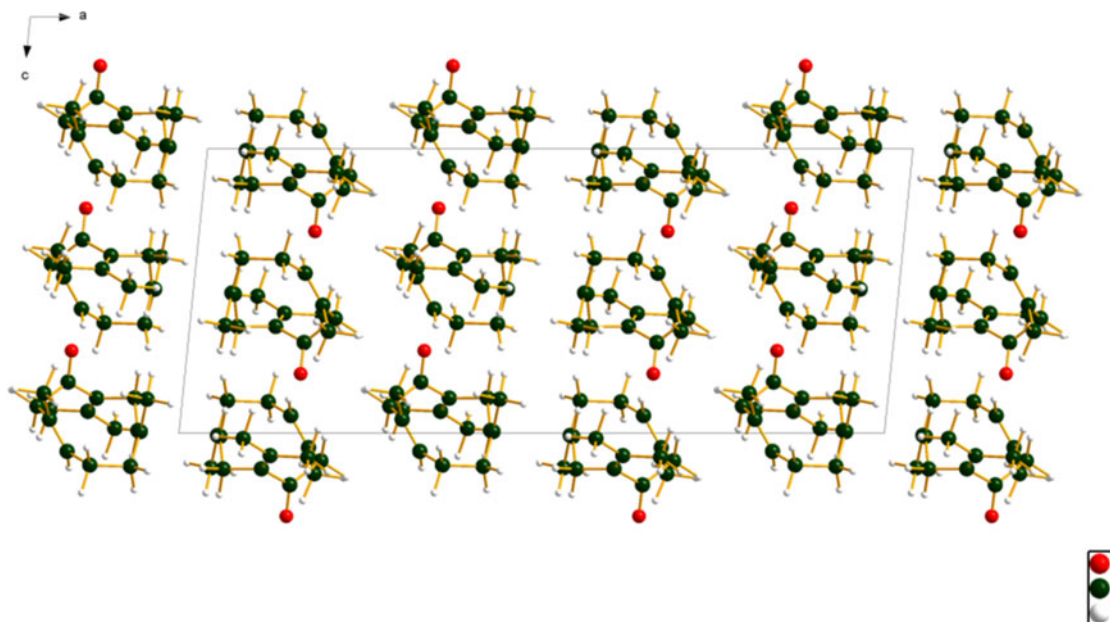
Figure 6. The crystal structure of germacrone Form II, viewed down the *b*-axis.
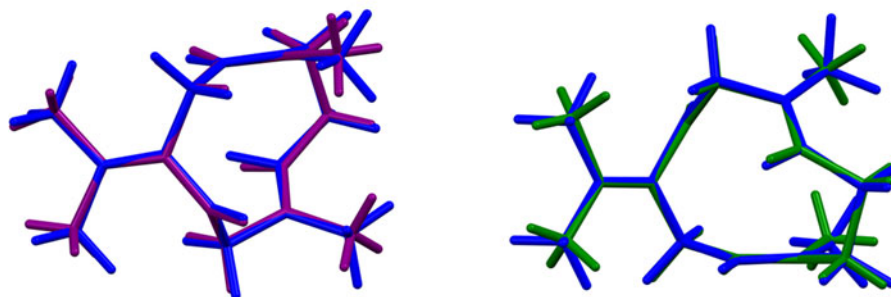
Figure 7. Comparison of the germacrone molecule in Form II (blue) with molecule 1 in the FIQLOG structure (purple, left) and molecule 2 (green, right).

structures (van de Streek and Neumann, 2014). This discussion concentrates on the DFT-optimized structure. The asymmetric unit (with atom numbering) is illustrated in Figure 5, and the crystal structure is presented in Figure 6. The crystal structure (Figure 6) indicates discrete molecules, and no particularly strong intermolecular interactions are apparent.

The rms Cartesian displacements between the germacrone molecule in this $C2/c$ structure and the two independent molecules in the Form I FIQLOG Pc structure are 0.079 and 0.79 Å (Figure 7). The ADDSYM module of PLATON (Spek, 2009) suggests that the symmetry of FIQLOG is $P2/c$, and checkCIF yields many alerts for this structure. The FIQLOG cell is about half the volume of the current one, but the angles differ (Table I). The structures exhibit many similarities (Figure 8), but the powder patterns (Figure 2) clearly show that they are different. VASP geometry optimizations for both this polymorph and FIQLOG indicate that this new polymorph is 0.55 kcal mol^{-1} cell^{-1} lower in energy, but this difference is within the expected error of such calculations. The two forms must be considered equivalent in energy.

All of the bond distances and angles fall within the normal ranges indicated by a Mercury/Mogul geometry check (Macrae *et al.*, 2020). The O1–C10–C4–C5 and O1–C10–

C4–C12 torsion angles (−56.2 and 123.9°, respectively) are flagged as unusual, and they are truly unusual. The unusual value is illustrated for O1–C10–C4–C12 (the two torsion angles are not independent) in Figure 9. These angles reflect the arrangement of the carbonyl and dimethylvinylidene groups, which are indeed an unusual pairing.

Quantum chemical geometry optimization of the germacrone molecule (DFT/B3LYP/6-31G*/water) using Spartan '18 (Wavefunction, 2020) indicated that the observed conformation is only 0.9 kcal mol^{-1} higher in energy than the local

TABLE I. Lattice parameters of germacrone polymorphs

Structure	FIQLOG (Type I)	This Work (Type II)
Space Group	*Pc*	*C2/c*
a, Å	13.573(2)	26.0073(4)
2*a*	27.146	
b, Å	9.8474(11)	9.84381(11)
c, Å	10.5451(12)	10.53725(13)
β, °	105.595(2)	95.7525(11)
V, Å^3	1357.56	2684.06(4)
2*V*	2715.12	1.0806
ρ, g cm^{-1}	1.0683	
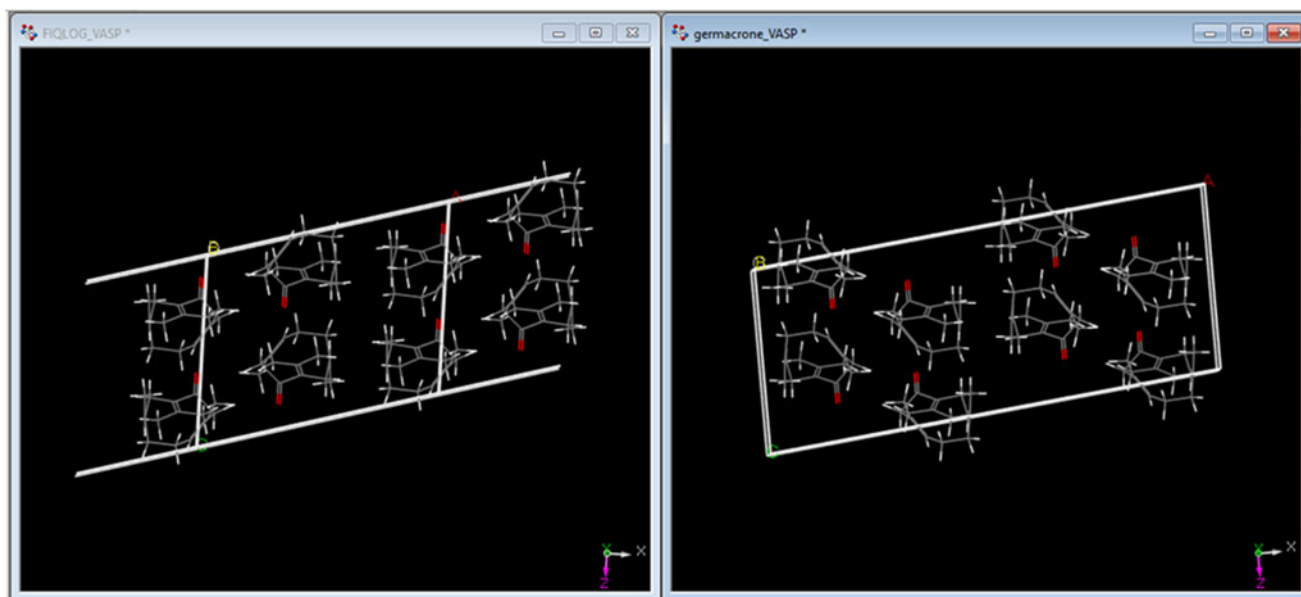
Figure 8. Comparison of the Form I FIQLOG and Form II crystal structures of germacrone.

minimum, and that the molecule is in the global minimum-energy conformation in the solid state.

Analysis of the contributions to the total crystal energy of the structure using the Forcite module of Materials Studio (Dassault, 2021) suggests that torsion distortion terms dominate the intramolecular deformation energy, though bond and angle distortion terms are also significant. The intermolecular energy is dominated by van der Waals attractions and electrostatic attractions, which in this force field analysis also include hydrogen bonds. The hydrogen bonds are better analyzed using the results of the DFT calculation.

There are no traditional hydrogen bonds in the structure, but the oxygen atom O1 acts as an acceptor in four C–H⋯O

hydrogen bonds (Table II). Two of these bonds are intramolecular. The Mulliken overlap populations indicate the presence of many, even weaker, intermolecular interactions.

The volume enclosed by the Hirshfeld surface (Figure 10; Hirshfeld, 1977; Turner et al., 2017) is 330.17 Å^3, 98.41% of 1/8 the unit cell volume. The packing density is thus fairly typical. The only significant close contact (red in Figure 10) involves a hydrogen bond. The volume/non-hydrogen atom is larger than normal, at 20.9 Å^3.

The Bravais–Friedel–Donnay–Harker (Bravais, 1866; Friedel, 1907; Donnay and Harker, 1937) morphology using Mercury (Macrae et al., 2020) suggests that we might expect fairly isotropic morphology for germacrone. No preferred
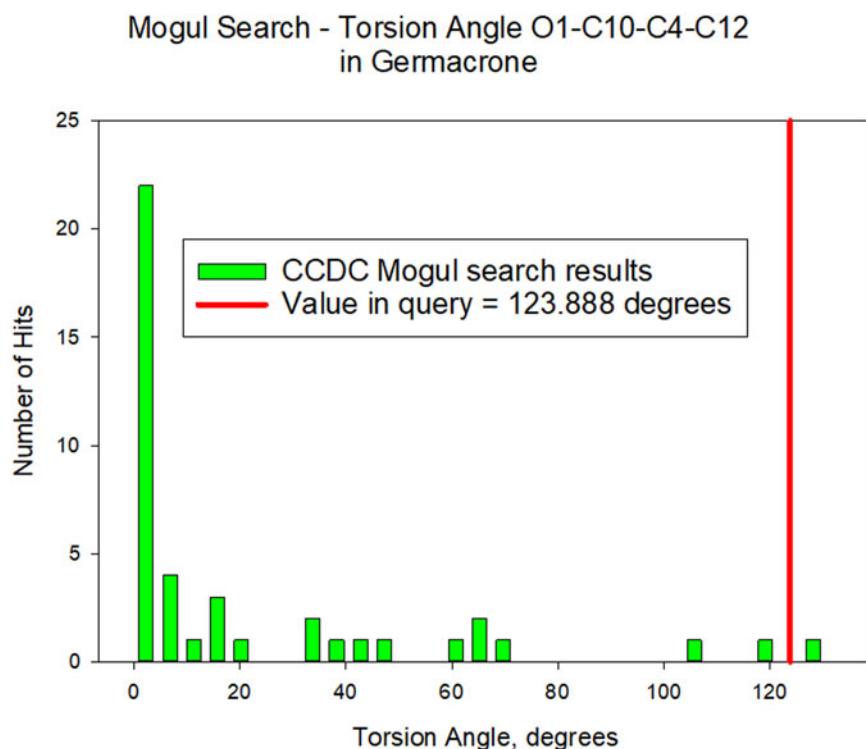
Figure 9. Comparison of the O1–C10–C4–C12 torsion angle in germacrone to the distribution of similar torsion angles indicated by a Mogul search.

TABLE II. Hydrogen bonds (CRYSTAL17) in germacrone.

H-Bond	D-H (Å)	H⋯A (Å)	D⋯A (Å)	D-H⋯A (°)	Overlap (e)
C14–H20⋯O1	1.102	2.473[a]	3.182	120.8	0.012
C5–H38⋯O1	1.100	2.604[a]	2.995	99.9	0.010
C16–H30⋯O1	1.102	2.545	3.301	124.8	0.010
C11–H33⋯O1	1.096	2.755	3.812	161.9	0.010

[a]Intamolecular.
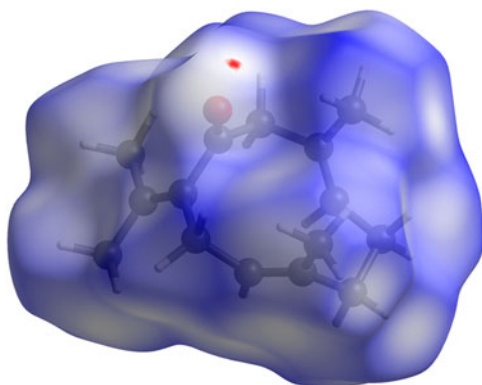
Figure 10. The Hirshfeld surface of germacrone Form II, calculated using *CrystalExplorer17* (Turner *et al.*, 2017). Intermolecular contacts longer than the sums of the van der Waals radii are colored blue, and contacts shorter than the sums of the radii are colored red. Contacts equal to the sums of radii are white.

orientation model was necessary for this rotated capillary specimen. The powder pattern of Type II germacrone from this synchrotron data set has been submitted to ICDD for inclusion in the Powder Diffraction File.

IV. DEPOSITED DATA

The supplementary material for this article, which includes the Crystallographic Information Framework (CIF) files containing the results of the Rietveld refinement (including the raw data) and the DFT geometry optimization was deposited with the ICDD. The data can be requested at info@icdd.com.

CONFLICTS OF INTEREST

The authors have no conflicts of interest to declare.

Altomare, A., Cuocci, C., Giacovazzo, C., Moliterni, A., Rizzi, R., Corriero, N., and Falcicchio, A. (2013). "EXPO2013: a kit of tools for phasing crystal structures from powder data," J. Appl. Crystallogr. 46, 1231–1235.

Antao, S. M., Hassan, I., Wang, J., Lee, P. L., and Toby, B. H. (2008). "State-of-the-art high-resolution powder X-ray diffraction (HRPXRD) illustrated with Rietveld refinement of quartz, sodalite, tremolite, and meionite," Can. Mineral. 46, 1501–1509.

Barrero, A. F., Mar Herrador, M., Arteaga, P., and Catalán, J. V. (2008). "Germacrone: occurrence, synthesis, chemical transformations and biological properties," Nat. Prod. Commun. 3, 567–576.

Bravais, A. (1866). *Etudes Cristallographiques* (Gauthier Villars, Paris).

Bruno, I. J., Cole, J. C., Kessler, M., Luo, J., Motherwell, W. D. S., Purkis, L. H., Smith, B. R., Taylor, R., Cooper, R. I., Harris, S. E., and Orpen, A. G. (2004). "Retrieval of crystallographically-derived molecular geometry information," J. Chem. Inf. Comput. Sci. 44, 2133–2144.

Clardy, J. C. and Lobkovsky, E. (1998). "Germacra-1(10),4,7(11)-trien-8-one," CSD Communication; Refcode FIQLOG.

Dassault Systèmes (2021). *Materials Studio 2021* (BIOVIA, San Diego, CA).

Donnay, J. D. H. and Harker, D. (1937). "A new law of crystal morphology extending the law of Bravais," Am. Mineral. 22, 446–447.

Dovesi, R., Erba, A., Orlando, R., Zicovich-Wilson, C. M., Civalleri, B., Maschio, L., Rerat, M., Casassa, S., Baima, J., Salustro, S., and Kirtman, B. (2018). "Quantum-mechanical condensed matter simulations with CRYSTAL," WIREs Comput. Mol. Sci. 8, e1360.

Friedel, G. (1907). "Etudes sur la loi de Bravais," Bull. Soc. Fr. Mineral. 30, 326–455.

Gates-Rector, S. and Blanton, T. (2019). "The Powder Diffraction File: a quality materials characterization database," Powd. Diffr. 39(4), 352–360.

Gatti, C., Saunders, V. R., and Roetti, C. (1994). "Crystal-field effects on the topological properties of the electron-density in molecular crystals - the case of urea," J. Chem. Phys. 101, 10686–10696.

Groom, C. R., Bruno, I. J., Lightfoot, M. P., and Ward, S. C. (2016). "The Cambridge Structural Database," Acta Crystallogr. Sect. B: Struct. Sci., Cryst. Eng. Mater. 72, 171–179.

Hirshfeld, F. L. (1977). "Bonded-atom fragments for describing molecular charge densities," Theor. Chem. Acta 44, 129–138.

Jacobsson, U., Norin, T., Weber, M., and Tsankova, E. (1985). "The configuration and conformation of isogermacrone. The significance of crossed conformations in olefinic cyclisations," Tetrahedron 41, 2033–2036. doi:10.1016/S0040-4020(01)96572-X.

Kaduk, J. A., Crowder, C. E., Zhong, K., Fawcett, T. G., and Suchomel, M. R. (2014). "Crystal structure of atomoxetine hydrochloride (Strattera), $C_{17}H_{22}NOCl$," Powd. Diffr. 29(3), 269–273.

Kim, S., Chen, J., Cheng, T., Gindulyte, A., He, J., He, S., Li, Q., Shoemaker, B. A., Thiessen, P. A., Yu, B., Zaslavsky, L., Zhang, J., and Bolton, E. E. (2019). "PubChem 2019 update: improved access to chemical data," Nucleic Acids Res. 47(D1), D1102–D1109. doi:10.1093/nar/gky1033.

Kresse, G. and Furthmüller, J. (1996). "Efficiency of ab-initio total energy calculations for metals and semiconductors using a plane-wave basis set," Comput. Mater. Sci. 6, 15–50.

Lee, P. L., Shu, D., Ramanathan, M., Preissner, C., Wang, J., Beno, M. A., Von Dreele, R. B., Ribaud, L., Kurtz, C., Antao, S. M., Jiao, X., and Toby, B. H. (2008). "A twelve-analyzer detector system for high-resolution powder diffraction," J. Synchrotron Radiat. 15(5), 427–432.

Macrae, C. F., Sovago, I., Cottrell, S. J., Galek, P. T. A., McCabe, P., Pidcock, E., Platings, M., Shields, G. P., Stevens, J. S., Towler, M., and Wood, P. A. (2020). "*Mercury 4.0*: from visualization to design and prediction," J. Appl. Crystallogr. 53, 226–235.

Materials Design (2016). *MedeA 2.20.4* (Materials Design Inc., Angel Fire, NM).

MDI (2021). *JADE Pro Version 8.1 (Computer Software)* (Materials Data, Livermore, CA, USA).

Rovesti, P. (1927). "Researches on the ethereal oil of *Geranium macrorrhizum* L. of Bulgaria," Notiz. chim. - ind. 2, 438–439.

Spek, A. L. (2009). "Structure validation in chemical crystallography," Acta Crystallogr. D 65, 148–155.

Sykes, R. A., McCabe, P., Allen, F. H., Battle, G. M., Bruno, I. J., and Wood, P. A. (2011). "New software for statistical analysis of Cambridge Structural Database data," J. Appl. Crystallogr. 44, 882–886.

Toby, B. H. and Von Dreele, R. B. (2013). "GSAS II: the genesis of a modern open source all purpose crystallography software package," J. Appl. Crystallogr. 46, 544–549.

Turner, M. J., McKinnon, J. J., Wolff, S. K., Grimwood, D. J., Spackman, P. R., Jayatilaka, D., and Spackman, M. A. (2017). *CrystalExplorer17*

(University of Western Australia). Available at: http://hirshfeldsurface.net.

van de Streek, J. and Neumann, M. A. (**2014**). "Validation of molecular crystal structures from powder diffraction data with dispersion-corrected density functional theory (DFT-D)," Acta Crystallogr. Sect. B: Struct. Sci., Cryst. Eng. Mater. **70**(6), 1020–1032.

Wang, J., Toby, B. H., Lee, P. L., Ribaud, L., Antao, S. M., Kurtz, C., Ramanathan, M., Von Dreele, R. B., and Beno, M. A. (**2008**). "A dedicated powder diffraction beamline at the advanced photon source: commissioning and early operational results," Rev. Sci. Instrum. **79**, 085105.

Wavefunction, Inc. (**2020**). Spartan '18 Version 1.4.5, Wavefunction Inc., 18401 Von Karman Ave., Suite 370, Irvine, CA 92612.